

# Electrical Resistivity Measurements in Cementitious Systems: Observations of Factors that Influence the Measurements

Robert Spragg (Corresponding Author)  
Graduate Research Assistant  
School of Civil Engineering, Purdue University  
550 Stadium Mall Drive  
West Lafayette, IN 47907-2051  
E-mail: [rspragg@purdue.edu](mailto:rspragg@purdue.edu)  
Phone: 765.494.7999

Chiara Villani  
Graduate Research Assistant  
School of Civil Engineering, Purdue University  
550 Stadium Mall Drive  
West Lafayette, IN 47907-2051  
E-mail: [cvillani@purdue.edu](mailto:cvillani@purdue.edu)  
Phone: 765.494.7999

Ken Snyder  
Leader, Supervisory Physicist  
Materials and Structural Systems Division  
National Institute of Standards and Technology  
100 Bureau Drive, Stop 8615  
Gaithersburg, MD 20899  
E-mail: [kenneth.snyder@nist.gov](mailto:kenneth.snyder@nist.gov)  
Phone: 301.975.4260

Dale Bentz  
Chemical Engineer  
Materials and Structural Systems Division  
National Institute of Standards and Technology  
100 Bureau Drive, Stop 8615  
Gaithersburg, MD 20899  
E-mail: [dale.bentz@nist.gov](mailto:dale.bentz@nist.gov)  
Phone: 301.975.5865

Jeffrey W. Bullard  
Materials Research Engineer  
Materials and Structural Systems Division  
National Institute of Standards and Technology  
100 Bureau Drive, Stop 8615  
Gaithersburg, MD 20899  
E-mail: [bullard@nist.gov](mailto:bullard@nist.gov)  
Phone: 301.975.5725

and

Jason Weiss  
Professor and Director of Pankow Materials Laboratory  
School of Civil Engineering, Purdue University  
550 Stadium Mall Drive  
West Lafayette, IN 47907-2051  
E-mail: [wjweiss@purdue.edu](mailto:wjweiss@purdue.edu)  
Phone: 765.494.2215

Submitted on July 31, 2012  
Re-submitted on November 16, 2012

Number of words: Body: 5,486; Figures: 2,000 (8x250) = Total: 7,486 (7,500 max)

## 1 ABSTRACT

2 The electrical resistivity of cement-based materials can be used as an indicator of its fluid transport properties, for  
3 use in quality control or for service life prediction. Although electrical tests have the advantage of being easy and  
4 rapid to perform, there are several key factors that can influence the results: 1) specimen geometry, 2) specimen  
5 temperature and 3) sample storage and conditioning. This paper addresses these issues and compares the  
6 measurements from several commercially available testing devices. First, the role of sample geometry is explained  
7 using three common geometries: surface, uniaxial and embedded electrodes. If the geometry is properly accounted  
8 for, measurements from different test geometries result in electrical resistivity values that are similar. Second, the  
9 role of sample temperature is discussed for both pore solution and uniaxial tests on cylinders. Third, the paper  
10 examines the importance of sample curing, storage, and conditioning. Sample storage and conditioning influences  
11 both the degree of hydration and the degree of saturation. The role of sample volume to solution volume is discussed  
12 as this may influence alkali leaching and pore solution conduction. This paper is intended to identify factors that  
13 influence the results of the rapid electrical test measurements and to help identify areas of future research that are  
14 needed so that robust specifications and standard test methods can be developed. This will enable electrical tests to  
15 be used to provide rapid, accurate, repeatable measurements of concrete's electrical properties.

## 16 BACKGROUND

### 17 A Brief Background of Electrical Tests in Cementitious Materials

18  
19 The electrical properties of cement-based materials have been investigated for nearly a century (1-3). One practical  
20 use of electrical measurements is the standard test that is commonly referred to as the rapid chloride permeability  
21 test (RCPT) (4). The RCPT measures the charge passed in a saturated sample over time when a constant voltage is  
22 applied. While widely used, the RCPT has a few shortcomings due to the relatively long sample preparation time, its  
23 destructive nature, and sample heating, which influences the results (5-8). Given these limitations, there is growing  
24 interest to develop non-destructive resistivity measurements that can replace the RCPT. The benefit of resistivity  
25 tests is that they can be low cost, repeatable, and rapid to perform (7, 9, 10). AASHTO and ASTM are in the process  
26 of developing standard test methods for surface resistivity testing (11, 12), and a multi-user study was conducted to  
27 assess the variability of two rapid resistivity tests (9, 10). While substantial research has focused on electrical  
28 methods over the last thirty years to describe material structure and transport properties (13-19), comparatively little  
29 research has focused on the role of sample conditioning and sample geometry. This paper serves to highlight  
30 important features that may need to be captured in the ongoing development of standard test methods.

### 31 The Influence of Sample Geometry

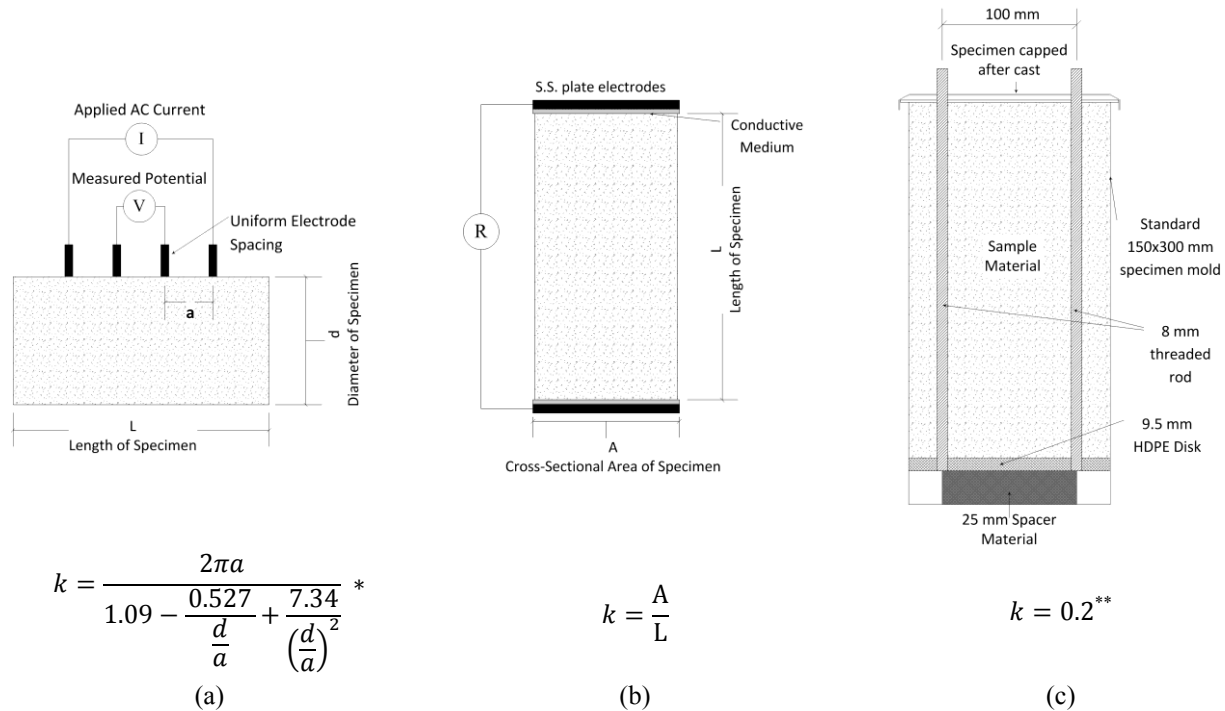
32  
33 Several different sample geometries have been used to measure the electrical properties of concrete. This section  
34 describes these geometries and discusses how they can be related to one another. The most commonly used  
35 geometries are shown in Figure 1. The first geometry is referred to as surface resistivity as shown in Figure 1a. The  
36 surface resistivity test uses a four electrode configuration where an alternating current is passed between the outer  
37 probes and the voltage is measured between the inner probes (In this paper a standard 100 mm diameter x 200 mm  
38 long cylinder specimen is used with a probe spacing of 38 mm (11)). The second geometry is typical of a uniaxial  
39 test where a set of plate electrodes are placed at the ends of a cylindrical specimen and used to measure the  
40 resistance through the cylinder, shown in Figure 1b. This test was conducted using the testing procedure described  
41 by Spragg et al. (10). The third geometry evaluated in this study used a set of embedded stainless steel rods (in this  
42 paper a standard 150 mm x 300 mm test cylinder was used with two embedded threaded rods as shown in Figure 1c  
43 and described by Castro et al. (20)).

44  
45 The tests highlighted in this study are based on measuring the electrical resistance between electrodes on a  
46 sample. This electrical resistance can be related to the geometry independent property known as resistivity using the  
47 approach shown in Equation 1:

$$48 \rho = Rk \quad (1)$$

49  
50 where  $\rho$  is the material resistivity,  $R$  is the measured resistance, and  $k$  is the geometry correction factor. This factor  
51 can be determined numerically (14, 21) or experimentally (10, 22) and is shown in Figure 1 for the geometries  
52 described above. In addition to these geometries, a wide range of electrode geometries and specimen sizes can be

1 used for this type of testing, provided the geometry factor can be determined, with examples provided in the  
 2 literature (14, 22-24).  
 3



4  
 5 **FIGURE 1** Testing geometries and geometric correction factors ( $k$ ) for cylindrical specimens: a) surface, b)  
 6 uniaxial, c) embedded electrode geometries. \*valid for specimens with  $d/a \leq 4.0$  and  $L/a \geq 5.0$ ; \*\* valid only for this  
 7 specimen geometry  
 8

### 9 The Influence of Sample Temperature

10 The temperature of the sample can substantially influence the measured resistivity (3, 25-28). An increase in the  
 11 temperature of the sample results in an increase in the mobility of the ions in the pore solution and a decrease in  
 12 measured resistivity. While several approaches have been proposed to account for temperature, the correction  
 13 investigated by the authors is a variation of the Arrhenius Law:  
 14

$$\rho_{t-Ref} = \rho_t \cdot \exp \left[ \frac{E_{A-Cond}}{R} \left( \frac{1}{T} - \frac{1}{T_{Ref}} \right) \right] \quad (2)$$

15 where  $\rho_{t-Ref}$  (ohm·m) is the resistivity at a reference temperature (23 °C in the U.S.),  $\rho_t$  (ohm·m) is the resistivity at  
 16 the testing temperature,  $E_{A-Cond}$  (kJ/mol) is the parameter known as the activation energy of conduction,  $R$  (8.314  
 17 J/(mol·K)) is the universal gas constant,  $T$  (K) is the testing temperature, and  $T_{Ref}$  (K) is the reference temperature  
 18 of 23 °C. Although changes in temperature can influence the rate of hydration of cement-based materials, this  
 19 correction is intended to account for the influence of temperature on the electrical measurements and hydration  
 20 effects are dealt with separately (28). This work will investigate the influence of temperature on both the pore  
 21 solution and sample resistivities.  
 22

### 24 The Influence of Sample Conditioning – Storage and Conditioning

25 Another important factor that can influence electrical measurements is how the samples are stored and conditioned.  
 26 To best illustrate this approach, the NIST developed Virtual Cement and Concrete Testing Laboratory (VCCTL)  
 27 model was used to simulate a mortar with a  $w/c$  of 0.42 with three curing conditions considered: 1) sealed during  
 28 curing and testing, 2) sealed during curing and saturated during testing, and 3) saturated during curing and testing.  
 29 Details on how these simulations were performed can be found in the literature (29, 30). There are two primary  
 30 factors that influence this response: the degree of hydration of the cement and the degree of saturation of the sample.

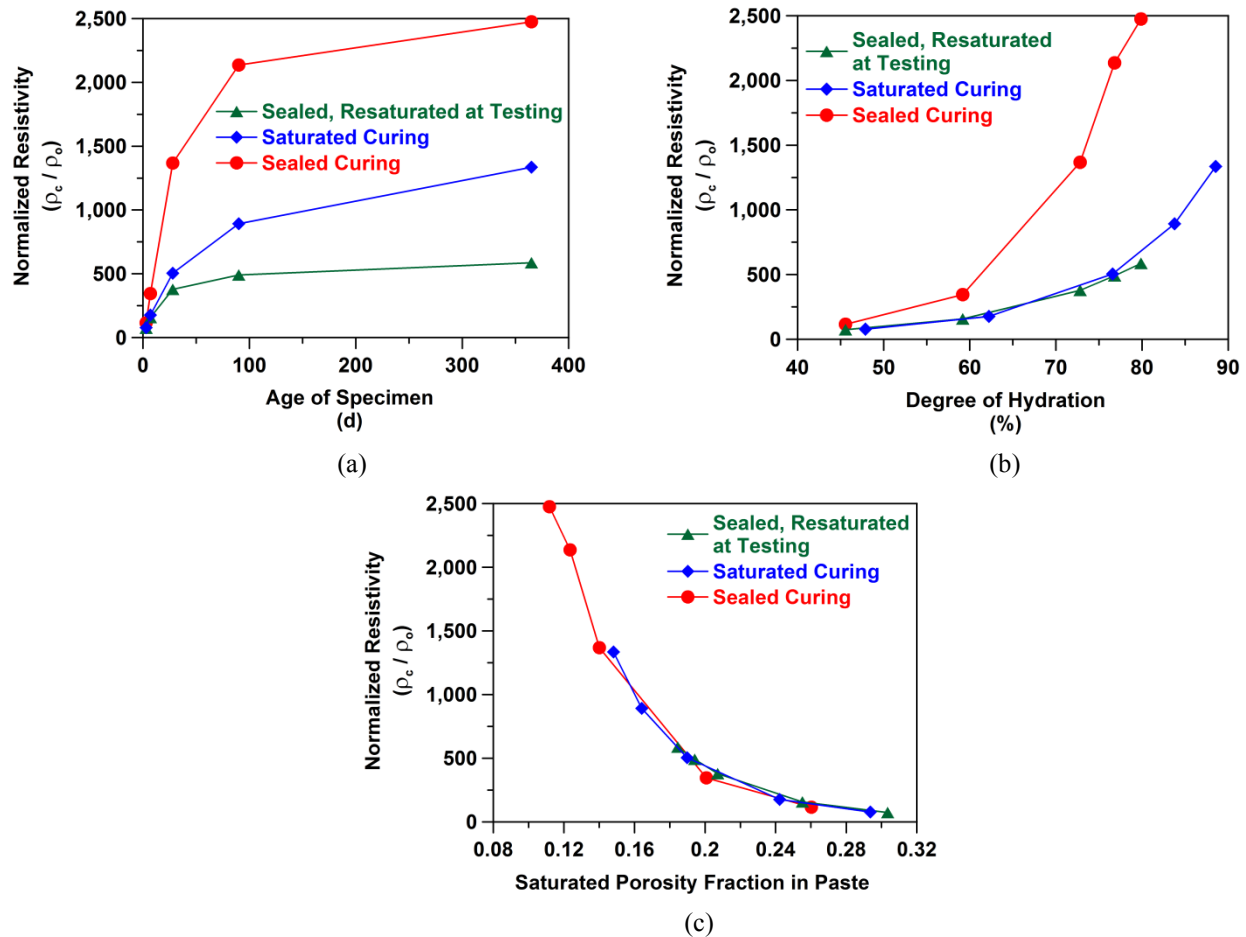
1           The uniaxial mortar resistivity ( $\rho_c$ ) values calculated from these simulations, normalized by the resistivity  
2 of the fluid in the pores ( $\rho_o$ ), are shown in [Figure 2](#). The sample that was sealed both during curing and testing had  
3 the greatest resistivity. The sample that was sealed during curing and saturated at the time of testing had the lowest  
4 resistivity. While the pore structure and degree of hydration of both samples is the same, the difference can be  
5 explained by the moisture content (or degree of saturation) of the sample. An approach has been proposed to account  
6 for changes in resistivity in partially saturated concrete using [Equation 3](#) (30):  
7

$$\rho^* = \rho S^{n-1+\delta} \quad (3)$$

8  
9 where  $\rho^*$  is the resistivity at saturation,  $\rho$  is the resistivity at a given level of saturation of  $S$  (which is between 0 and  
10 1),  $n$  is fitting parameter termed the saturation coefficient, and  $\delta$  describes the the ionic strength of the pore solution  
11 and how it changes during drying. For the mortar used in this study (the physical experiments), the degree of  
12 saturation was varied between 85 % and 100 % and it was observed that an exponent ( $n-1+\delta$ ) of 4.15 best fit the  
13 data, which compares well to the data presented by Weiss et al. (30) from the simulations.

14           [Figure 2](#) also shows that the storage of samples in lime water results in a greater degree of hydration than  
15 that achieved in samples that were sealed. The data points in [Figure 2b](#) provide evidence that different degrees of  
16 hydration occur due to sample conditioning, while [Figure 2a](#) presents these measurements at the same specimen age.  
17 This implies that storing a sample underwater in the lab may result in a substantially different degree of hydration  
18 than what may be occur in a field structure. It can be noticed that the sample that is continually saturated and the  
19 sample that is sealed and saturated at the time of testing have a similar resistivity for the same degree of hydration;  
20 however, the sample that is continually saturated has a higher degree of hydration at the same age. In [Figure 2c](#),  
21 these model results suggest that, for a given sample, the resistivity at any degree of saturation can be estimated from  
22 a single measurement, given that the relative change in the pore solution conductivity can also be predicted. These  
23 models also suggest that resistivity measurements can be evaluated in terms of the fraction of saturated porosity in  
24 the paste, as shown in [Figure 2c](#), with results similar to those reported by Weiss et al. (30).

25           It has also been hypothesized that for samples that are cured under saturated lime-water, the volume of  
26 solution in which the samples are stored can influence resistivity measurements. This may be due to possible pore  
27 solution concentration or dilution via leaching. This work will carefully investigate the influence of the volume of  
28 storage solution to sample size that is used for saturated lime-water curing.  
29  
30  
31  
32  
33  
34  
35  
36  
37  
38  
39  
40  
41



1 **FIGURE 2** VCCTL simulations of the same  $w/c=0.42$  mortar mixture evaluated for three curing conditions (data  
 2 are shown at ages of 3 d, 7 d, 28 d, 90 d and 365 d and are presented normalized by the resistivity of the fluid in the  
 3 pores).  
 4

## 5 MATERIALS

6 The samples described in this paper were made using a mortar and a paste, each with a water to cement ratio of 0.42  
 7 by mass. The mortar mixture consisted of 55 % aggregate by volume, made with a fine aggregate with a specific  
 8 gravity of 2.61 and an absorption capacity of 2.20 % by dry mass. A Type I ordinary portland cement with a Blaine  
 9 fineness of 375  $m^2/kg$ , a specific gravity of 3.17, and an estimated Bogue composition of 60 %  $C_3S$ , 10 %  $C_2S$ , 9 %  
 10  $C_3A$ , and 10 %  $C_4AF$  by mass was used. The cement contained an alkali content of 0.35%  $Na_2O$  and 0.77%  $K_2O$ .  
 11 Based upon the chemical composition, the ultimate theoretical heat release was calculated to be 512 J/g, using the  
 12 tabulated heat of hydration of each Bogue phase (31, 32).

13 This study evaluated samples that were stored in a lime-saturated solution. This solution was always used  
 14 at a lime dosage rate of 3.0 g / L of solution to ensure a saturated solution. At saturation, the solubility of pure  
 15 calcium hydroxide is 1.2 g / L of water.  
 16

## 17 EXPERIMENTAL EQUIPMENT USED FOR RESISTIVITY TESTING

18 Sample resistance was measured using four different commercially available resistivity meters. Each meter used an  
 19 alternating current (AC), but operated at a different frequency. The Proceq Resipod was used for surface resistivity  
 20 testing (Figure 1a) at a fixed probe tip spacing of 38 mm and uniaxial resistivity testing (Figures 1b) using the  
 21 uniaxial resistivity testing kit available from Proceq, and operating at a frequency of 40 Hz. The M.C. Miller 400D  
 22 was used in uniaxial resistivity testing (Figures 1b) at a frequency of 80 Hz. The uniaxial measurements (Figures 1b)  
 23 using the RCON meter were performed at a single frequency (1 KHz), with the exception of the equivalent circuit

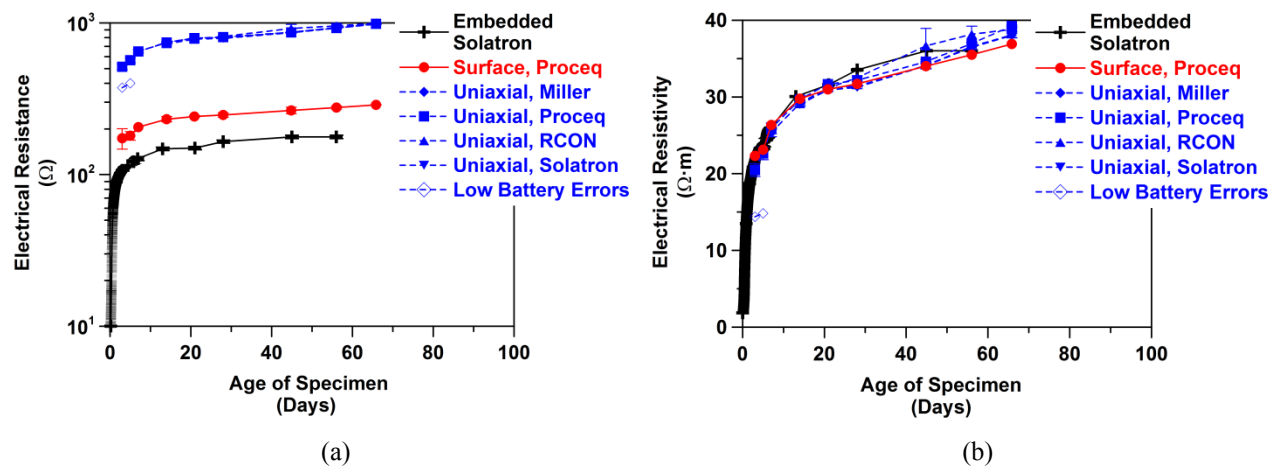
1 model discussed in Section 4.5. To quantify the effect of a single frequency measurement, the Solatron 1260A  
 2 impedance spectrometer across a frequency range of 1Hz to 10MHz.

## 4 EXPERIMENTAL RESULTS AND DISCUSSION

### 6 Corrections for Geometry

7 Measurements of electrical resistance were made on sealed specimens, i.e. specimens heat sealed in double plastic  
 8 bags between testing, and the results are shown in Figure 3a. It can be noticed that when the appropriate correction  
 9 for geometry is applied (using Equation 1 and values highlighted in Figure 1) to calculate the electrical resistivity,  
 10 the results obtained from different specimens of different geometries are quite comparable, as shown in Figure 3b.

11 It is interesting to note that a few of the early age uniaxial measurements using the Miller resistivity meter  
 12 (highlighted using hollow diamond symbols in the figure) show a much lower resistance. These lower measurements  
 13 were traced to low battery levels and when the battery was replaced for a second set of experiments, the results were  
 14 comparable with other experiments. This however shows the value in having a standard, unchanging reference  
 15 sample that can be used each day to confirm that the meter is working properly.



17 **FIGURE 3** Measurements conducted on sealed mortar specimens with different geometries for: a) resistance and  
 18 b) resistivity. Error bars represent the standard deviation of three specimens.

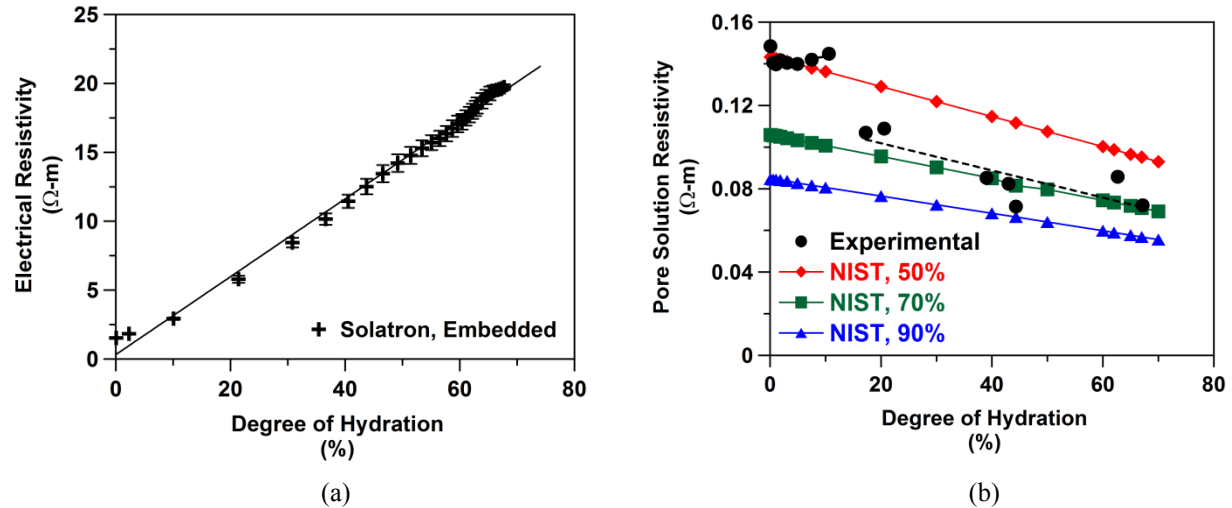
### 20 Pore Solution Contribution

21 The resistivity of the sealed mortar was measured and is plotted against the degree of hydration (DOH), determined  
 22 from isothermal calorimeter measurements (33), and shown in Figure 4a. The resistivity is nearly a linear function of  
 23 the DOH, which is similar to previously reported data (14, 20, 34).

24 The pore solution is the primary conducting phase in cement-based materials, and has a resistivity several  
 25 orders of magnitude lower than the solids and vapor phases (14). To study how the pore solution changes with  
 26 hydration, the pore solution was extracted from paste specimens with a  $w/c = 0.42$ . Solutions were extracted at ages  
 27 of 10 min, 1 h, 2 h, 3 h, 4 h, 5 h, 6 h, and 7 h while still in the fresh state by a Millipore pressure filtering system,  
 28 using nitrogen gas at pressures up to 200 kPa (35). Extractions performed on hardened samples were conducted at  
 29 ages of 1 d, 3 d, 5 d, and 7 d using a high pressure die at pressures up to 380 MPa as described by Barneyback et al.  
 30 (36). The extracted solutions were then measured for resistivity using a pore solution cell described by Castro (33).

31 The experimentally measured pore solutions were compared to a model (37) which was developed into an  
 32 online tool by Bentz (<http://concrete.nist.gov/poresolncalc.html>) (38). This model predicts the electrical properties of  
 33 the pore solution using only the masses of the water, cement and supplementary materials; the chemical composition  
 34 of those materials (i.e., their Na<sub>2</sub>O, K<sub>2</sub>O and SiO<sub>2</sub> mass percentages); and the estimated degree of hydration. The  
 35 model estimates the composition of the pore solution and then evaluates the electrical properties of this pore  
 36 solution. One assumption, however, that has to be made in this model is the proportion of alkalis that initially  
 37 dissolve in the solution. While a value of 75 % is a typical default value that can be employed, assumed values of  
 38 50 %, 70 %, and 90 % are shown in Figure 4b along with the experimental results. Initially, a value of 50 % of the  
 39 alkalis dissolving in solution appears appropriate; however, between a degree of hydration of 10 % and 20 % this

1 value suddenly increases to 70 %. It is interesting that this appears to relate to the shoulder of heat release curve that  
 2 was observed for this system and which generally relates to the renewed reaction of the calcium aluminate phase of  
 3 the cement. Several methods currently exist to rapidly assess the pore solution resistivity including pore solution  
 4 extraction, estimation using an approach like the NIST website, and embedded sensors (14, 20). Research is ongoing  
 5 to better understand the correlation between these results.



7 **FIGURE 4** Resistivity measurements: a) on sealed mortar specimens, where error bars represent the standard  
 8 deviation of three specimens and b) on extracted pore solution and compared to model results for different alkali  
 9 dissolution percentages.

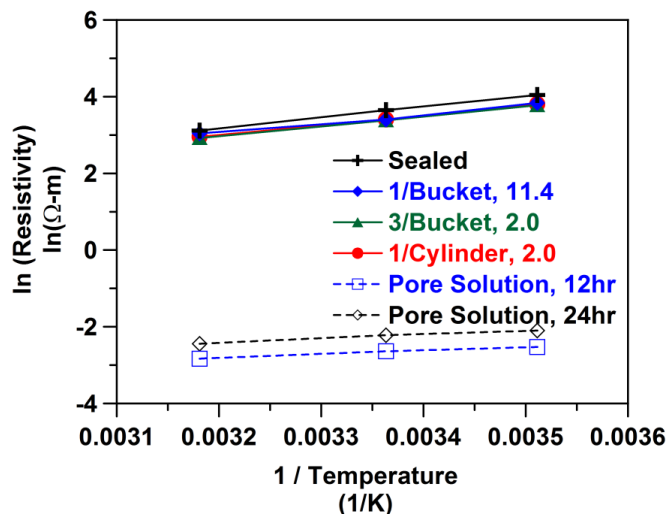
### 11 Influence of Temperature

12 Temperature can also influence the measured electrical response. For example, the resistivity measured using the  
 13 same mature sample can differ by as much as 80 % when the temperature of the sample fluctuates between 10 °C  
 14 and 45 °C. This is primarily due to the increased ionic mobility of the material's pore solution and can be described  
 15 using an Arrhenius approach (Equation 2).

16 The activation energy of conduction ( $E_{A-Cond}$ ), can be determined using the slope of a plot of the natural  
 17 logarithm of resistivity and the inverse of temperature as shown in Figure 5. The slope of the best fit line is  
 18 multiplied by the negative of the universal gas constant [ $-8.314 \text{ J}/(\text{mol}\cdot\text{K})$ ] to determine the activation energy of  
 19 conduction.

20 Figure 5 shows results for mature mortar cylinders (closed symbols) and extracted pore solution (open  
 21 symbols). The sealed specimens exhibit an activation energy of conduction of  $23.4 \pm 0.13 \text{ kJ/mol}$ , the specimens  
 22 stored in volume to solution ratio of 2.0 exhibit an average value of  $21.5 \pm 0.08 \text{ kJ/mol}$ , and the specimens stored in  
 23 a solution to sample ratio of 11.4 exhibit a value of  $19.9 \pm 0.42 \text{ kJ/mol}$ . Previously reported values for the activation  
 24 energy of conduction in mortar specimens have included  $18.7 \pm 2.5 \text{ kJ/mol}$ , values in excess of 20, and ranges of 16  
 25 – 30 kJ/mol (14, 26, 28). The activation energy of conduction was also measured on pore solution extracted from  
 26 specimens at ages of 12 h and 24 h, resulting in values of  $8.7 \pm 0.18 \text{ kJ/mol}$  and  $7.7 \pm 0.12 \text{ kJ/mol}$  respectively.  
 27 Previously reported results for synthetic and extracted solutions have ranged from 8.98 kJ/mol to 13.8 kJ/mol (14,  
 28 20, 28).

29 This difference between measured activation energies of conduction obtained on extracted pore solution  
 30 and uniaxial cylinders appear to suggest the microstructure of a material can also influence these measurements, as  
 31 previously noted by Rajabipour (14). This may be due in part to the confinement provided by the pore space, pore  
 32 constriction, surface/absorption effects, or changes in the pore fluid volume during heating and cooling; however  
 33 additional work is needed to fully understand the reasons for these changes.



1  
2 **FIGURE 5** Activation energy of conduction measured on uniaxial samples (closed points) and extracted pore  
3 solution (hollow points) using electrical impedance spectroscopy. Linear fits show an average  $R^2$  of 0.996.  
4

### 5 **Influence of Sample Storage and Conditioning**

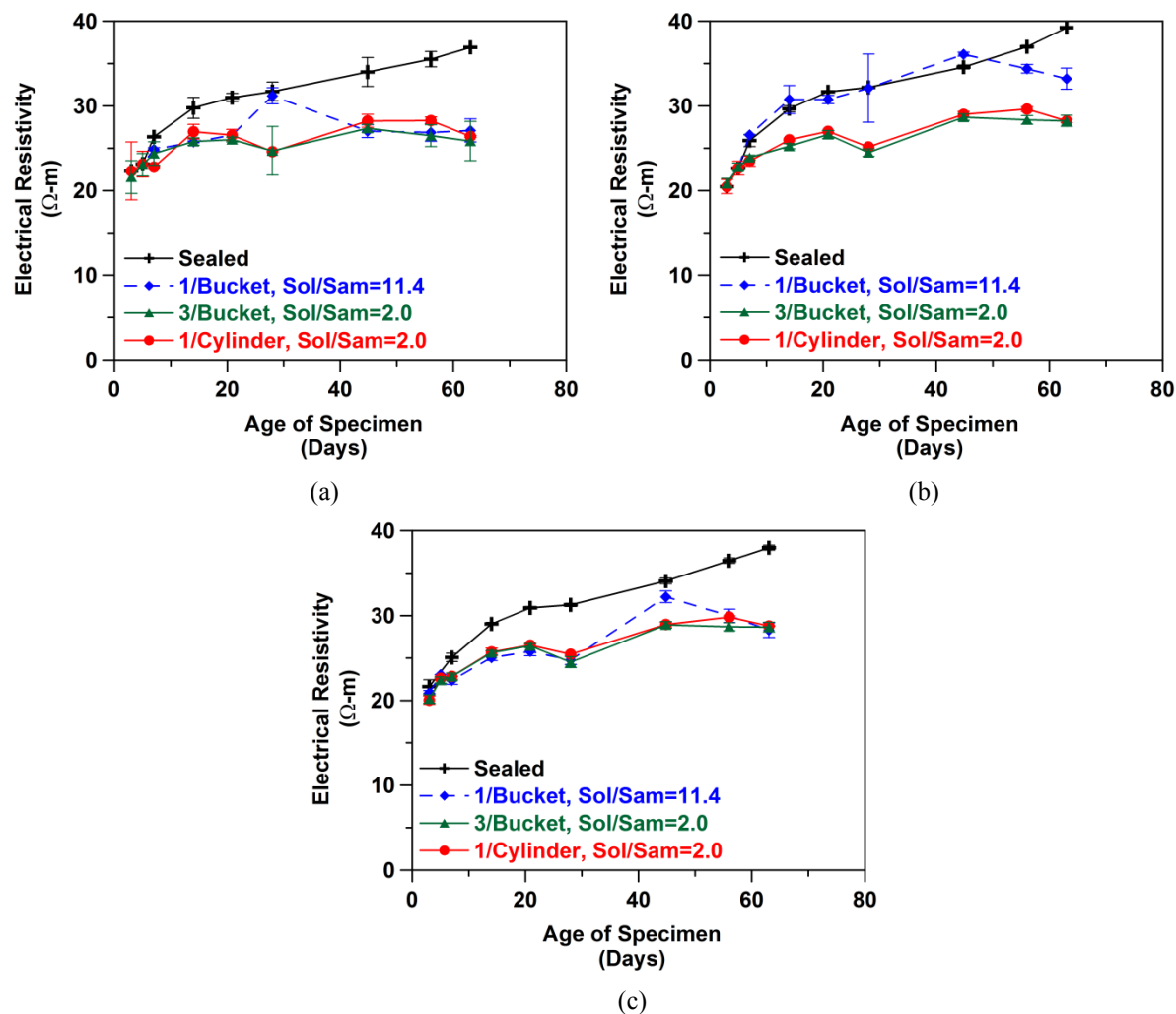
6 As previously mentioned, the conduction of the electrical current occurs primarily through the pore fluid in the  
7 cementitious system. While the pore solution changes during hydration, the pore solution may also change if ions  
8 leach from the sample to the surrounding solution. As such, a series of tests was conducted where the ratios of the  
9 volumes of the lime saturated solution to sample (Sol/Sam) varied (2.0 and 11.4). The Sol/Sam of 2.0 can be  
10 obtained when using a standard 100 mm x 200 mm testing specimen by using: one specimen in a standard 150 mm x  
11 300 mm mold or 3 samples in 5-gallon bucket. The Sol/Sam of 11.4 can be obtained when using a single specimen  
12 in a 5-gallon bucket.

13 The samples were stored in a lime-saturated solution as described above and was monitored for electrical  
14 resistivity. The nominal resistivity of the lime saturated solution is 12.6  $\Omega$ -m. The measured resistivity of solution  
15 in the system where the Sol/Sam was 11.4 initially increased to a value of 16  $\Omega$ -m at approximately two weeks,  
16 before it began to decrease, reaching 13.8  $\Omega$ -m after 2 months. The measured resistivity of solution in the system  
17 where the Sol/Sam was 2.0 initially decreased to a value of 2  $\Omega$ -m by approximately one week, while it slowly  
18 decreased to 1.3  $\Omega$ -m after 2 months. Initial data seems to suggest this is due to ion leaching and dilution effects, but  
19 future research will investigate this in more detail.

20 In addition to monitoring the resistivity of the solution, resistivity measurements were measured on the  
21 sample using: surface and uniaxial geometries at a frequency of 40 Hz, and uniaxial resistivity measured over a  
22 range of frequencies. Figure 6 shows the resistivity for the samples measured using the different storage conditions.  
23 It can be noticed that the resistivity of the sealed sample is higher than the samples stored in the solution with a  
24 Sol/Sam of 2.0. This can be explained by the fact that the samples in solution have a higher degree of saturation.

25 It is interesting to note that the samples stored with Sol/Sam of 11.4 where the resistivity was measured at  
26 low frequency more closely resembles the measurements conducted on sealed samples than other samples that are  
27 lime-water cured (Figure 6b). Testing at a variable frequency (Figure 6c) provides similar results for specimens  
28 stored in both Sol/Sam with less than 1 % difference.  
29

30 At early ages up to 7 d, the surface resistivity measurements have more variability than the uniaxial  
31 measurements, evidenced by standard deviations that are up to 2.7 times higher for surface measures using 8  
32 samples. (Figure 6a and 6b), while at later ages the effect of storage solution volume seems to be reduced. This can  
33 likely be attributed to the effects of leaching of surface alkalis in both solution volumes. The results obtained to date  
34 suggest that at later ages, the influence of storage solution volume on surface measurements and uniaxial  
35 measurements at variable frequencies (Figures 6a and 6c) is generally within the variability of the measurement,  
36 while uniaxial measurements at fixed frequencies show differences from 10 to 30 % between storage solutions  
37 (Figure 6b).  
38



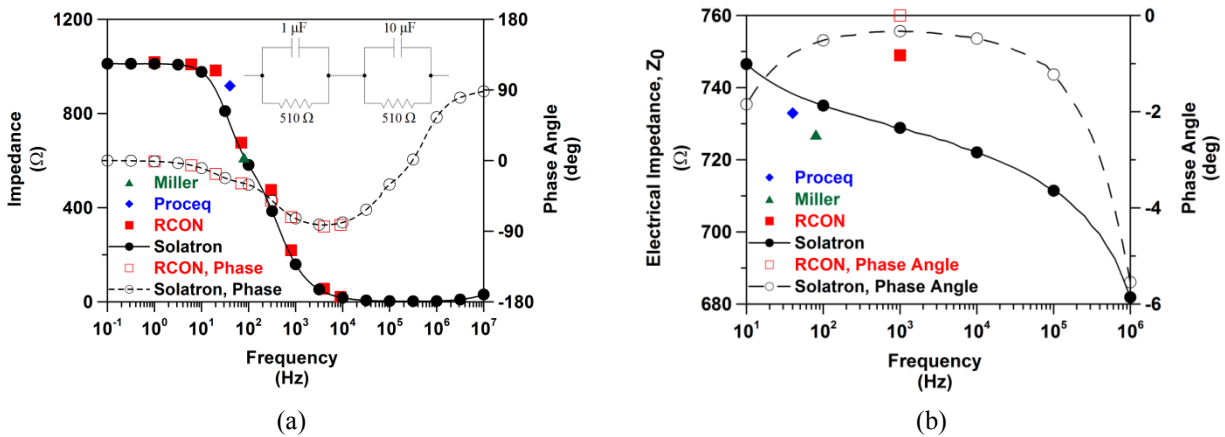
1 **FIGURE 6** Resistivity measurements using differing solution to sample ratios: a) surface b) uniaxial 40 kHz  
 2 frequency and c.) uniaxial multi-frequency measurements. Error bars represent the standard deviation of a minimum  
 3 of three specimens.  
 4

### 5 Influence of Measurement Frequency on Total Impedance

6 Because saturated cementitious systems behave like resistor-capacitor circuits, resulting in a phase difference  
 7 between the applied current and the measured voltage (impedance), and there is a noticeable difference in  
 8 impedance at different frequencies; the real component of the impedance at zero phase angle is the true uniaxial  
 9 resistance. Because the phase is (almost never) zero, the meters report the total impedance  $Z_o$ ; the real and  
 10 imaginary components added in quadrature. To compare the response of the different meters, an electrical circuit  
 11 (Figure 7) was used and the responses are shown in Figure 7a; the Proceq was configured for uniaxial resistivity.  
 12 The Solatron meter provides a response over a wide range of frequencies, and the values are shown using circular  
 13 symbols (every 10<sup>th</sup> symbol is shown). The Miller and Proceq meters were tested at a single frequency and are  
 14 shown by the triangle and the diamond-shaped symbols, respectively. The phase angle, shown with hollow points  
 15 and dashed lines is also used to highlight the frequency dependence. While the measured response of the meters  
 16 shown in Figure 7a compare well with one another, the data demonstrate why the resistance reported from each unit  
 17 will not be the same, as they are measured at different frequencies.

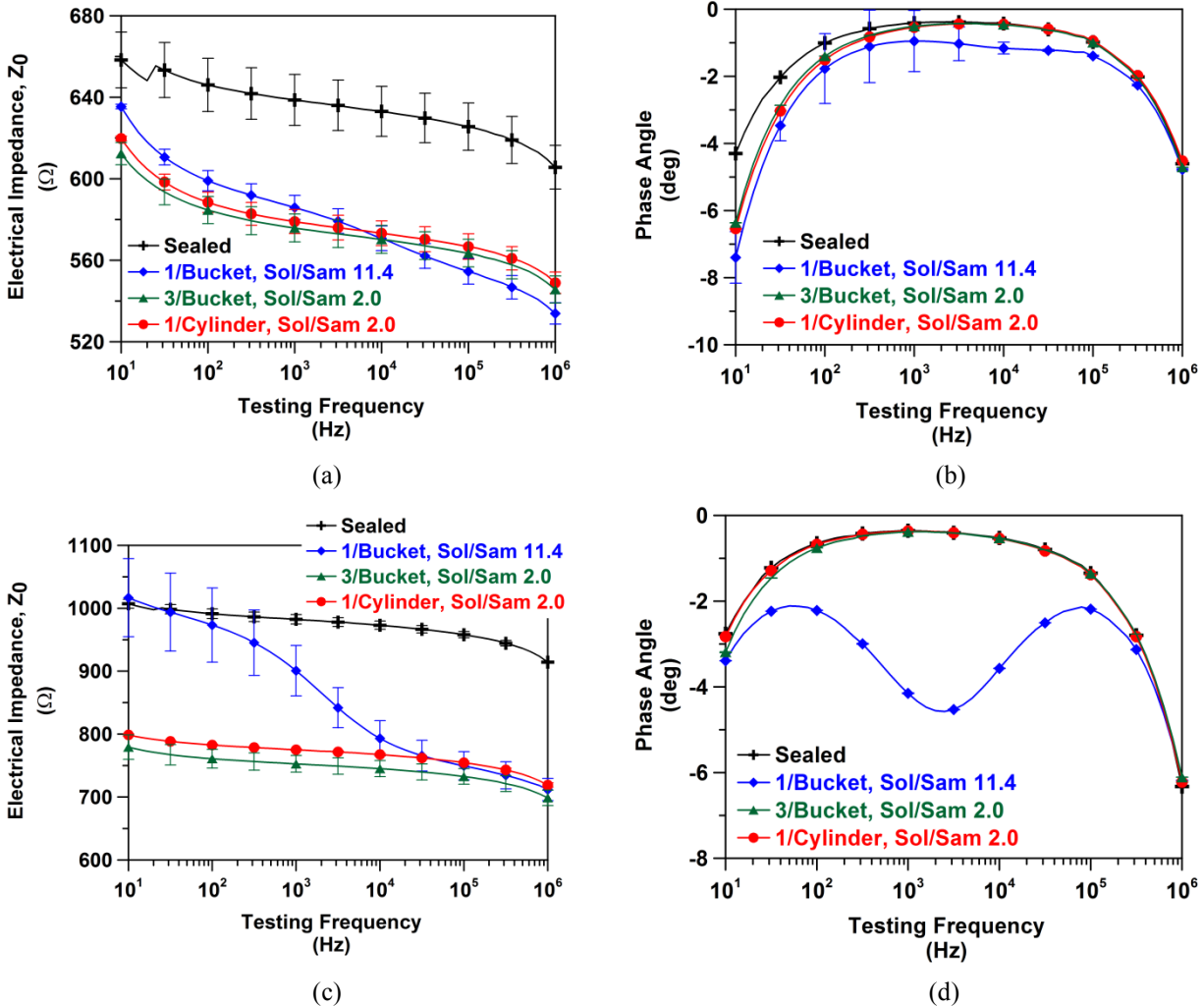
18 The frequency dependence of the electrical response also exists in uniaxial mortar specimens as shown for  
 19 a specimen stored in Sol/Sam of 2.0 conditions at an age of 45 d in Figure 7b. While there is not a significant  
 20 difference between the measurements of the single frequency meters and the impedance spectra, there is a difference  
 21 seen in the resistivity that would be reported among these different meters. This can be explained through the  
 22 influence of frequency, while the two fixed meters operate in the range of 80 Hz to 100 Hz, the measurements used

1 by the Solatron have the lowest imaginary impedance at 794 Hz which would be where the uniaxial resistance  
 2 would be reported. Note that the Proceq and Miller devices report values approximately 5 % lower than the true  
 3 uniaxial value determined by the Solartron.  
 4



5 **FIGURE 7** The influence of frequency on total impedance illustrated through the use of a) equivalent circuit and  
 6 b) a uniaxial measurement on a mortar cylinder at an age of 45 d.

7  
 8 A variable frequency was also used to interpret uniaxial resistivity measurements for samples stored using  
 9 different sample to solution volumes. It can be noticed that the frequency responses change as the specimen ages, as  
 10 shown in Figure 8 for 5 d and 65 d samples, respectively. Specimens with a larger Sol/Sam exhibit more variability  
 11 between samples, which is even more pronounced at later ages. This may be explained by the impedance response  
 12 across the frequency range. This is especially evident in the phase angle measurements, where the larger storage  
 13 volume appears to have two local minima contrasted with the other specimen conditions, which is largely  
 14 pronounced at later ages, but can also be seen even as early as five days.  
 15  
 16  
 17  
 18  
 19  
 20  
 21  
 22  
 23  
 24  
 25  
 26  
 27  
 28



1 **FIGURE 8** Frequency and phase angle responses of specimens with different Sol/Sam: a and b) 5 d and c and d)  
 2 65 d. Error bars represent the standard deviation of three specimens.  
 3  
 4

## 5 CONCLUSIONS

6 There are several key factors that should be considered in standardizing tests for the electrical resistivity of cement-  
 7 based materials. First, different specimen geometries can be used; however, the measured resistance should be  
 8 converted to the resistivity using an appropriate geometry correction factor. Second, the temperature of the specimen  
 9 during the test can also influence resistivity measurements, so a relatively narrow temperature range of the test  
 10 specimens (e.g.,  $\pm 2$  °C) should be specified in standard test methods. The temperature dependence can be partially  
 11 attributed to the increased mobility of the ionic species of the pore solution. It was shown that both pore solution  
 12 resistivity and specimen resistivity measurements follow an Arrhenius relationship, with different activation  
 13 energies of conduction ( $E_{A-Cond}$ ). Third, it was shown that sample storage and conditioning is also important, as it  
 14 can influence the degree of hydration, the degree of saturation, and the pore structure and solution through leaching.  
 15 Differences in resistivity can develop due to sample storage conditions (sealed versus saturated). It was noticed that  
 16 when hardened specimens were stored in different solutions of different volumes inconsistent results were obtained.  
 17 This appears to be related to pore solution dilution which appears to alter the measured frequency spectra. As such,  
 18 testing at variable frequencies has the ability to reduce these effects, but for testing at a fixed frequency the solution  
 19 volume surrounding the sample should be tightly controlled. A solution to sample volume ratio of 2.0 appears to be  
 20 an appropriate recommendation at this time. Future studies are underway to investigate this potential dilution effect  
 21 and the potential gradients that develop in the material that can lead to sample inhomogeneity (39).

## 1 ACKNOWLEDGEMENTS

2 This work was supported in part by the Joint Transportation Research Program administered by the Indiana  
3 Department of Transportation and Purdue University (Project SPR 3509). The contents of this paper reflect the  
4 views of the authors, who are responsible for the facts and the accuracy of the data presented herein, and do not  
5 necessarily reflect the official views or policies of the Federal Highway Administration and the Indiana Department  
6 of Transportation, nor do the contents constitute a standard, specification, or regulation. The authors thank Giatec  
7 Scientific for supplying a unit for testing.  
8

## 9 DISCLAIMER

10 Certain commercial products are identified in this paper to specify the materials used and procedures employed. In  
11 no case does such identification imply endorsement or recommendation by the National Institute of Standards and  
12 Technology or Purdue University, nor does it indicate that the products are necessarily the best available for the  
13 purpose.  
14

## 15 REFERENCES

- 16 1. Shimizu, Y. An electrical method for measuring the setting time of portland cement. *Mill Section of Concrete*,  
17 Vol. 32, No. 5, 1928, pp 111-113.
- 18 2. Calleja, J. Effect of current frequency on measurement of electrical resistance of cement pastes. *Journal of the*  
19 *American Concrete Institute*, Vol. 24, No. 4, 1952, pp 329-332.
- 20 3. Whittington, H. W., J. McCarter and M. C. Forde. The conduction of electricity through concrete. *Magazine of*  
21 *Concrete Research*, Vol. 33, No. 114, 1981, pp 48-60.
- 22 4. ASTM C1202, 2010, *Standard test method for electrical indication of concrete's ability to resist chloride ion*  
23 *penetration*, ASTM International, West Conshohocken, PA, doi: 10.1520/C1202-10.
- 24 5. Julio-Betancourt, G. A. and R. D. Hooton. Study of the Joule effect on rapid chloride permeability values and  
25 evaluation of related electrical properties of concretes. *Cement and Concrete Research*, Vol. 34, No. 6, 2004, pp  
26 1007-1015.
- 27 6. Snyder, K. A., C. Ferraris, N. S. Martys and E. J. Garboczi. Using impedance spectroscopy to assess the  
28 viability of the rapid chloride test for determining concrete conductivity. *Journal of Research of the National*  
29 *Institute of Standards and Technology (USA)*, Vol. 105, No. 4, 2000, pp 497-509.
- 30 7. Rupnow, T. D. and P. Icenogle. *Evaluation of surface resistivity measurements as an alternative to the rapid*  
31 *chloride permeability test for quality assurance and acceptance*. Publication FHWA/LA.11/479. 2011.
- 32 8. Spragg, R. P., J. Weiss and T. Nantung. *Proposal for the development of a resistivity method for the Indiana*  
33 *Department of Transportation*. 2012.
- 34 9. Paredes, M., N. M. Jackson, A. El Safty, J. Dryden, J. Josen, H. Lerma and J. Hersey. Precision Statements for  
35 the Surface Resistivity of Water Cured Concrete Cylinders in the Laboratory. *Advances in Civil Engineering*  
36 *Materials*, Vol. 1, No. 1, 2012.
- 37 10. Spragg, R. P., J. Castro, T. Nantung, M. Paredes and J. Weiss. Variability Analysis of the Bulk Resistivity  
38 Measured Using Concrete Cylinders. *Advances in Civil Engineering Materials*, Vol. 1, No. 1, 2012.
- 39 11. AASHTO TP95-11, *Standard Method of Test for Surface Resistivity Indication of Concrete's Ability to Resist*  
40 *Chloride Ion Penetration*, American Association of State Highway and Transportation Officials, Washington,  
41 D.C.
- 42 12. WK 37880, 2012, *Draft Standard Test Method for Measuring the Surface Resistivity of Hardened Concrete*  
43 *Cylinders using the Wenner Four-Electrode Method*, ASTM International, West Conshohocken, PA.
- 44 13. Christensen, B. J., R. T. Coverdale, R. A. Olson, S. J. Ford, E. J. Garboczi, H. M. Jennings and T. O. Mason.  
45 Impedance spectroscopy of hydrating cement-based materials: measurement, interpretation, and application.  
46 *Journal of the American Ceramic Society*, Vol. 77, No. 11, 1994, pp 2789-2804.
- 47 14. Rajabipour, F. *In situ electrical sensing and material health monitoring in concrete structures*. Ph.D. Purdue  
48 University, 2006.
- 49 15. Archie, G. E. The electrical resistivity log as an aid in determining some reservoir characteristics. *SPE Reprint*  
50 *Series*, 2003, pp 9-16.
- 51 16. Garboczi, E. J. Permeability, diffusivity, and microstructural parameters: A critical review. *Cement and*  
52 *Concrete Research*, Vol. 20, No. 4, 1990, pp 591-601.
- 53 17. Snyder, K. A. The relationship between the formation factor and the diffusion coefficient of porous materials  
54 saturated with concentrated electrolytes: Theoretical and experimental considerations. *Concrete Science and*  
55 *Engineering*, Vol. 3, No. 12, 2001, pp 216-224.

- 1 18. McLachlan, D. S., M. Blaszkiewicz and R. E. Newnham. Electrical resistivity of composites. *Journal of the*  
2 *American Ceramic Society*, Vol. 73, No. 8, 1990, pp 2187-2203.
- 3 19. Xie, P., P. Gu, A. Zu and J. J. Beaudoin. A Rationalized A.C. Impedance Model for the Microstructural  
4 Characterization of Hydrating Cement Systems. *Cement and Concrete Research*, Vol. 23, No. 2, 1992, pp 359-  
5 367.
- 6 20. Castro, J., R. Spragg, P. Kompore and W. J. Weiss. *Portland Cement Concrete Pavement Permeability*  
7 *Performance*. Publication FHWA/IN/JTRP-2010/29. 2010.
- 8 21. Morris, W., E. I. Moreno and A. A. Sagues. Practical evaluation of resistivity of concrete in test cylinders using  
9 a Wenner array probe. *Cement and Concrete Research*, Vol. 26, No. 12, 1996, pp 1779-1787.
- 10 22. Castro, J., R. Spragg and J. Weiss. Water Absorption and Electrical Conductivity for Internally Cured Mortars  
11 with a W/C between 0.30 and 0.45. *Journal of Materials in Civil Engineering*, Vol. In press, 2011.
- 12 23. Peled, A., J. M. Torrents, T. O. Mason, S. P. Shah and E. J. Garboczi. Electrical Impedance Spectra to Monitor  
13 Damage *ACI Materials Journal*, Vol. 98, No. 4, 2001, pp 313-322.
- 14 24. Weiss, W. J. *Prediction of early-age shrinkage cracking in concrete elements*. Ph.D. Northwestern University,  
15 1999.
- 16 25. Hammond, E. and T. D. Robson. Comparison of electrical properties of various cements and concretes. I-II. *The*  
17 *Engineer*, Vol. 199, 1955, pp 78-80.
- 18 26. McCarter, W. J., G. Starrs and T. M. Chrisp. Electrical conductivity, diffusion, and permeability of Portland  
19 cement-based mortars. *Cement and Concrete Research*, Vol. 30, No. 9, 2000, pp 1395-1400.
- 20 27. Nokken, M., A. Boddy, X. Wu and R. D. Hooton. Effects of temperature, chemical, and mineral admixtures on  
21 the electrical conductivity of concrete. *Journal of ASTM International*, Vol. 5, No. 5, 2008.
- 22 28. Sant, G., F. Rajabipour and J. Weiss. The influence of temperature on electrical conductivity measurements and  
23 maturity predictions in cementitious materials during hydration. *Indian Concrete Journal*, Vol. 82, 2008, pp 7-  
24 16.
- 25 29. Bullard, J. W., C. F. Ferraris, E. J. Garboczi, N. S. Martys, P. E. Stutzman and J. E. Terrill. Chapter 10: Virtual  
26 Cement and Concrete. In *Innovations in Portland Cement Manufacturing*, Portland Cement Association,  
27 Skokie, IL, 2008.
- 28 30. Weiss, W. J., K. A. Snyder, J. W. Bullard and D. P. Bentz. Using a Saturation Function to Interpret the  
29 Electrical Properties of Partially Saturated Concrete *Accepted to Journal of Materials in Civil Engineering*,  
30 2012.
- 31 31. Taylor, H. F. W. *Cement Chemistry*. Thomas Telford, London, 1997.
- 32 32. Fukuhara, M., S. Goto, K. Asaga, M. Daimon and R. Kondo. Mechanisms and kinetics of C<sub>4</sub>AF hydration with  
33 gypsum. *Cement and Concrete Research*, Vol. 11, No. 3, 1981, pp 407-414.
- 34 33. Castro, J. *Moisture Transport in Cement Based Materials: Application to Transport Tests and Internal Curing*.  
35 Ph.D. Purdue University, 2011.
- 36 34. Feng, X., E. J. Garboczi, J. W. Bullard, D. P. Bentz, K. A. Snyder, P. E. Stutzman and T. O. Mason. *Expanding*  
37 *a tool for predicting chloride diffusivity in concrete so it can be used by manufacturers to evaluate the*  
38 *durability of concrete made with blended cements. Part I: Characterizing blended cement materials*. 2004.
- 39 35. Penko, M. *Some early hydration processes in cement pastes as monitored by liquid phase composition*  
40 *measurements*. Purdue University, 1983.
- 41 36. Barneyback, S. and S. Diamond. Expression and analysis of pore fluids from hardened cement pastes and  
42 mortars. *Cement and Concrete Research*, Vol. 11, No. 2, 1981, pp 279-285.
- 43 37. Snyder, K. A., X. Feng, B. D. Keen and T. O. Mason. Estimating the electrical conductivity of cement paste  
44 pore solutions from OH, K, and Na concentrations. *Cement and Concrete Research*, Vol. 33, No. 6, 2003, pp  
45 793-798.
- 46 38. Bentz, D. P. A virtual rapid chloride permeability test. *Cement and Concrete Composites*, Vol. 29, No. 10,  
47 2007, pp 723-731.
- 48 39. Spragg, R. P. *The Rapid Assessment of Transport Properties of Cementitious Materials Using Electrical*  
49 *Methods*. M.S.C.E. Purdue University, 2013.
- 50
- 51